HHS Public Access

Author manuscript

Science. Author manuscript; available in PMC 2017 August 24.

Published in final edited form as:

Science. 2017 January 27; 355(6323): 403–407. doi:10.1126/science.aaf6407.

A SUMO-ubiquitin relay recruits proteasomes to chromosome axes to regulate meiotic recombination

H. B. D. Prasada Rao[1,2], **Huanyu Qiao**[1,2], **Shubhang K. Bhatt**[2], **Logan R. J. Bailey**[2], **Hung D. Tran**[2], **Sarah L. Bourne**[2], **Wendy Qiu**[2], **Anusha Deshpande**[2], **Ajay N. Sharma**[2], **Connor J. Beebout**[2], **Roberto J. Pezza**[3], and **Neil Hunter**[1,2,4,5,*]

[1]Howard Hughes Medical Institute, University of California, Davis, CA 95616, USA

[2]Department of Microbiology and Molecular Genetics, University of California, Davis, CA 95616, USA

[3]Cell Cycle and Cancer Biology Research Program, Oklahoma Medical Research Foundation, Oklahoma City, OK 73104, USA

[4]Department of Molecular and Cellular Biology, University of California, Davis, CA 95616, USA

[5]Department of Cell Biology and Human Anatomy, University of California, Davis, CA 95616, USA

Abstract

Meiosis produces haploid gametes through a succession of chromosomal events, including pairing, synapsis, and recombination. Mechanisms that orchestrate these events remain poorly understood. We found that the SUMO (small ubiquitin-like modifier)–modification and ubiquitin-proteasome systems regulate the major events of meiotic prophase in mouse. Interdependent localization of SUMO, ubiquitin, and proteasomes along chromosome axes was mediated largely by RNF212 and HEI10, two E3 ligases that are also essential for crossover recombination. RNF212-dependent SUMO conjugation effected a checkpointlike process that stalls recombination by rendering the turnover of a subset of recombination factors dependent on HEI10-mediated ubiquitylation. We propose that SUMO conjugation establishes a precondition for designating crossover sites via selective protein stabilization. Thus, meiotic chromosome axes are hubs for regulated proteolysis via SUMO-dependent control of the ubiquitin-proteasome system.

Meiosis halves the chromosome complement via two successive rounds of cell division. Accurate segregation of homologous chromosomes (homologs) during the first meiotic division requires their connection by chiasmata—the conjunction of crossing over and sister-chromatid cohesion (1). Chiasma formation is the culmination of an elaborate series of interdependent events that include programmed recombination and the pairing and synapsis of homologs. Each homolog comprises two sister chromatids, which are organized into

*Corresponding author. nhunter@ucdavis.edu.

SUPPLEMENTARY MATERIALS

www.sciencemag.org/content/355/6323/403/suppl/DC1

Materials and Methods

Figs. S1 to S15

References (29–39)

arrays of chromatin loops connected to a common core or axis. Pairing and synapsis are promoted by homologous recombination, which occurs in physical and functional association with these axes. As meiosis progresses, axes align and become connected along their lengths to form synaptonemal complexes (SCs).

The SUMO (small ubiquitin-like modifier)–modification (SMS) and ubiquitin-proteasome (UPS) systems are key regulators of cellular proteostasis (2, 3) and are implicated in various aspects of meiotic prophase (4–9). However, their roles remain poorly characterized, especially in mammalian meiosis. To obtain cytological evidence that the SMS and UPS regulate axis-associated events, we analyzed the localization of SUMO, ubiquitin, and proteasomes along surface-spread chromosomes from mouse spermatocytes (Fig. 1 and figs. S1 to S3).

The SUMO1 and SUMO2/3 isoforms localized to axes during zygonema, as chromosomes underwent synapsis, forming punctate patterns of ~200 immunostaining foci (Fig. 1, A and B, and fig. S1). Superresolution structured illumination microscopy (SIM) revealed that SUMO was present on both unsynapsed and synapsed axes; axial, supra-axial (extending into adjacent chromatin), and SC central-region staining could be discerned (Fig. 1A and fig. S1). General axis staining disappeared after synapsis completed and cells entered pachynema (Fig. 1, A and B, and fig. S1). Subsequently, SUMO accumulated on centromeric heterochromatin and the XY chromatin (sex body) (10). Prominent axis staining of ubiquitin was also detected during zygonema but persisted throughout pachynema (Fig. 1, A and B, and fig. S2). SIM revealed that most ubiquitin foci localized to axes, but SC central-region staining was occasionally discerned (Fig. 1A and fig. S2). Ubiquitin also accumulated along axes of the sex chromosomes during zygonema and early pachynema, before spreading to the entire XY chromatin (11). Prominent staining of centromeric heterochromatin was not seen for ubiquitin, but general chromatin staining became apparent after mid-pachynema (Fig. 1, A and B, and fig. S2). Abundant recruitment of proteasomes along axes also occurred during zygonema (Fig. 1, A and B, and fig. S3) and persisted throughout pachynema and diplonema, when chromosomes desynapsed. By SIM, proteasome foci were largely axis associated, but less frequent SC central-region staining was also seen. Sex body, centromeric, and general chromatin staining were not detected. This subchromosomal recruitment of proteasomes to meiotic chromosome axes, which appears to be an evolutionarily conserved feature of meiosis [see accompanying paper (12)], predicts that axis-associated ubiquitin should include chains linked through lysine 48; this inference was confirmed by using linkage-specific ubiquitin antibodies (fig. S2) (13).

These immunostaining results suggest that the SMS and UPS regulate axis-associated events via protein degradation. To test this, we exploited short-term culture of testis cell suspensions (14) and chemical inhibitors of SUMO conjugation (2-DO8) (15), ubiquitin activation (PYR41) (16), or proteasomal degradation (MG132) (Fig. 2 and figs. S4 to S6). All three inhibitors caused dramatic increases in large extra-chromosomal aggregates containing SYCP3 and SYCP2, two meiosis-specific components of chromosome axes (17) (Fig. 2, A and B, and fig. S4). Large increases in synapsis defects were also observed (Fig. 2, A and C, and fig. S4). Thus, the SMS and UPS modulate axis assembly and formation and/or maintenance of synapsis in mammalian meiosis. Phenotypes of *Saccharomyces*

cerevisiae and *Caenorhabditis elegans* mutants defective for proteasome (12) or CSN/COP9 signalosome (18) functions imply that a role for the UPS in synapsis is likely to be conserved.

Absent inhibitors, cultured spermatocytes continued to progress through meiotic prophase (14), manifested by a reduction in pachytene cells and a corresponding increase in diplotene cells after 24 hours (Fig. 2D). Treatment with 2-DO8, PYR41, or MG132 blocked progression out of pachynema (Fig. 2D). Moreover, precocious progression into metaphase I triggered by the phosphatase inhibitor, okadaic acid, was blocked by 2-DO8, PYR41, and MG132 (fig. S5). Thus, the SMS and UPS are important for both entry and exit from the pachytene stage of meiosis.

A dependent relationship between the SMS and UPS was revealed by immunostaining analysis of inhibitor-treated spermatocytes. 2-DO8 diminished not only SUMO staining (Fig. 2, E and F, and fig. S6) but also axis-associated ubiquitin and proteasomes (Fig. 2, E and F), raising the possibility that SUMO-modified proteins become substrates for the UPS. Indeed, SUMO staining accumulated and persisted when ubiquitylation was inhibited, whereas proteasome recruitment remained defective (Fig. 2, E and F, and fig. S6). Furthermore, chromosomal staining of both SUMO and ubiquitin became abundant and persistent when proteasomes were inhibited (Fig. 2, E and F, and fig. S6).

Effects of inhibiting the SMS and UPS on recombination were investigated by immunostaining for markers representing each step of the pathway (Fig. 3 and figs. S7 and S8). MEI4 is required for initiation of recombination by DNA double-strand breaks (DSBs) and localizes as several hundred foci along axes during leptonema and early zygonema (19) (Fig. 3A). In untreated spermatocytes, MEI4 foci decreased between early and mid-zygonema (Fig. 3B). Inhibition of SUMO, ubiquitin, or proteasomes did not alter MEI4 foci in early zygonema, but numbers remained aberrantly high in mid-zygonema and, to a lesser extent, late zygonema (Fig. 3, A and B), implying that the SMS and UPS promote MEI4 turnover. RAD51 is a RecA family protein that promotes DNA pairing and strand exchange (20). In control cells, RAD51 foci were abundant during early zygonema and diminished throughout zygonema as recombination proceeded (Fig. 3, C and D, and fig. S7). Initial numbers of RAD51 foci were not changed by drug treatments, which suggests that DSB numbers and assembly of RAD51 complexes were unaffected; however, turnover of RAD51 was defective. SUMO inhibition decreased RAD51 foci in mid-zygonema by ~61%, implying accelerated turnover (Fig. 3, C and D, and fig. S7). In contrast, when ubiquitylation or proteasomes where inhibited, RAD51 foci remained high, consistent with defective turnover (Fig. 3, C and D, and fig. S7). Analogous results were obtained for meiosis-specific RecA homolog, DMC1 (fig. S7).

As chromosomes synapse, a distinct set of recombination factors associate with homolog axes, including ZMM proteins, which are required for efficient synapsis and crossing over (1). The DNA helicase, MER3, stabilizes nascent DNA strand-exchange intermediates. Inhibition of the SMS or UPS had dramatically different effects on MER3 dynamics: SUMO inhibition halved the numbers of MER3 foci in late zygotene nuclei, whereas ubiquitin and proteasome inhibition increased MER3 foci ~2.5-fold (Fig. 3, E and F). Similar trends were

seen for three other ZMM members (TEX11, MSH4, and RNF212) and single-strand DNA binding protein RPA, which localizes to recombination sites with timing similar to that of the ZMMs (fig. S8). Finally, we analyzed the localization of ubiquitin-ligase, HEI10, which specifically marked crossover sites during mid/late pachynema (Fig. 3, G and H) (21). HEI10 focus numbers increased only very slightly after inhibition of the SMS or UPS (Fig. 3, G and H). However, SUMO inhibition resulted in significantly brighter HEI10 foci (fig. S9), implying that SUMOylation negatively regulates HEI10 accumulation. Together, inhibitor studies indicate general roles for the SMS and UPS in regulating turnover of recombination factors and, more specifically, reveal opposing effects on the chromosomal dynamics of ZMMs and associated factors, with SMS promoting stabilization and UPS promoting turnover. This interpretation is supported by genetic analysis below.

Two RING-family E3 ligases are essential for crossing over in mouse (21, 22). RNF212 is inferred to catalyze SUMO conjugation and promotes selective stabilization of the ZMM factor, MutSg, at the minority of recombination sites that will mature into crossovers (~10% in mouse) (22). By contrast, HEI10 stimulates ubiquitylation and antagonizes RNF212 by promoting its turnover from synapsed chromosomes (21). To understand the relationships between RNF212, HEI10, and the axis-localized SUMO, ubiquitin, and proteasomes described here, immunostaining was performed on spermatocyte chromosomes from *Rnf212*$^{-/-}$ and *Hei10*$^{-/-}$ single-mutant mice and the *Rnf212*$^{-/-}$ *Hei10*$^{-/-}$ double mutant (Fig. 4); in subsequent analyses, spermatocyte chromosome spreads were prepared directly from testes, without intervening cell culture. Axis SUMOylation was largely dependent on RNF212 (Fig. 4, A and B, and fig. S10). However, accumulation of SUMO at the sex body and centromeric heterochromatin were still observed in *Rnf212*$^{-/-}$ nuclei (fig. S10), indicating that RNF212 promotes SUMO conjugation specifically along chromosome axes. On the contrary, SUMO was abundant and persistent along synapsed chromosomes in *Hei10*$^{-/-}$ spermatocytes, and high levels were now detected throughout pachynema (Fig. 4, A and B, and fig. S10). Analysis of the *Rnf212*$^{-/-}$ *Hei10*$^{-/-}$ double mutant revealed that this hyper-SUMO phenotype was RNF212 dependent (Fig. 4, A and B). Thus, RNF212 and HEI10 mediate, respectively, formation and turnover of axis-associated SUMO conjugates. Although the fungus, *Sordaria macrospora*, lacks a RNF212 homolog, its HEI10-like protein has also been shown to modulate SUMO levels along SCs (23).

Consistent with a model in which RNF212-mediated SUMO conjugation creates substrates for HEI10-dependent proteasomal degradation, axis-localized ubiquitin and the recruitment of proteasomes were diminished in *Rnf212*$^{-/-}$and *Hei10*$^{-/-}$ single mutants and the *Rnf212*$^{-/-}$ *Hei10*$^{-/-}$ double mutant (Fig. 4, C to F, and fig. S10); ubiquitin staining of sex chromosomes appeared unaffected. Analogous observations were made for female meiosis (fig. S11). Together, these results point to the same pathway relationships inferred from inhibitor studies, with RNF212-dependent SUMOylation establishing a requirement for ubiquitin-dependent proteolysis via HEI10. However, unlike general inhibition of the SMS and UPS, *Rnf212*$^{-/-}$ and *Hei10*$^{-/-}$ mutations do not cause overt defects in synapsis or progression to metaphase (21, 22). Thus, the SUMO-ubiquitin-proteasome relay defined by RNF212 and HEI10 appears dedicated to the regulation of post-synapsis steps of meiotic recombination.

To better understand how recombination is regulated by the RNF212-HEI10 pathway, we analyzed the same set of markers described above for chemical inhibition experiments (Fig. 4, G to L, and figs. S12 and S13). Although pan-inhibition caused abnormally high numbers of MEI4 foci to persist through zygotene (Fig. 3, A and B), mutation of *Rnf212* and/or *Hei10* did not (Fig. 4, G and H) indicating that MEI4 turnover does not require the RNF212-HEI10 pathway. In contrast, RAD51 turnover was strongly dependent on HEI10; in *Hei10*$^{-/-}$ nuclei, high numbers of RAD51 foci persisted throughout zygonema and pachynema (Fig. 4, I and J, and fig. S12). Moreover, persistence of RAD51 was RNF212 dependent as foci decreased to wild-type levels in the *Rnf212*$^{-/-}$ *Hei10*$^{-/-}$ double mutant. Unlike global UPS inhibition, which impeded turnover of both RAD51 and DMC1, Hei10$^{-/-}$ mutation did not slow the disappearance of DMC1 foci (fig. S12). Thus, turnover of the two RecA homologs involves distinct branches of the UPS, distinguished by their dependency on HEI10. This result is consonant with studies showing that DMC1 is the dominant DNA strand-exchange activity during meiosis, whereas RAD51 plays an essential supporting role that does not require its catalytic activity (24, 25). Differential regulation of DMC1 and RAD51 by the RNF212-HEI10 pathway suggests that RAD51 also plays a later role in meiotic recombination.

We extended our previous studies showing that *Rnf212* and *Hei10* mutations differentially affect turnover of the ZMM factor, MutSγ, with faster turnover in the absence of RNF212 and persistence when HEI10 was absent (21, 22) (fig. S13). Differential effects of *Rnf212*$^{-/-}$ and *Hei10*$^{-/-}$ mutations were also observed for MER3 (Fig. 4, K and L) and a third ZMM factor, TEX11 (fig. S13). In all three cases, persistence of high numbers of ZMM foci seen in *Hei10*$^{-/-}$ mutant nuclei was largely RNF212 dependent. We also confirmed that the general DSB marker, γH2AX, persists along synapsed chromosomes of *Hei10*$^{-/-}$ spermatocytes (21) and showed that persistence was dependent on RNF212 (fig. S13).

Although crossing over is abolished in *Rnf212*$^{-/-}$ and *Hei10*$^{-/-}$ mutants, overall DSB repair remains efficient (21, 22). Moreover, unlike pan-inhibition of SUMO and ubiquitin conjugation (Fig. 2), *Rnf212*$^{-/-}$ and *Hei10*$^{-/-}$ mutations do not cause synapsis defects, which could cause secondary defects in recombination. These considerations support direct roles for the SMS and UPS in regulating recombination. Consistently, subsets of RNF212 and HEI10 foci precisely localize to recombination sites (21, 22). However, costaining for the general recombination marker, RPA, and SUMO, ubiquitin, or proteasomes revealed only 28 to 38% colocalization (fig. S14). Thus, the bulk of chromosomal SUMO, ubiquitin, and proteasomes does not stably localize with recombination sites, suggesting that the branch of the SUMO-UPS pathway defined here may regulate recombination indirectly via chromosome axes. That said, most RPA foci localized immediately adjacent to, or interdigitated with, SUMO, ubiquitin, or proteasome signals (fig. S14). Moreover, modification of recombination factors by SUMO or ubiquitin and interaction with proteasomes are expected to be transient.

In conclusion, the SMS and UPS function coordinately to facilitate major transitions of meiotic prophase including axis morphogenesis, homolog synapsis and recombination (fig. S15). RNF212 and HEI10 define an axis-associated, SUMO-ubiquitin-proteasome relay that mediates turnover of the subset of recombination factors that act after DMC1-promoted

homolog pairing. This stage marks a key regulatory transition during which a small number of crossover sites are designated from the large pool of ongoing recombination events in such a way that each chromosome pair acquires at least one chiasma (fig. S15) (26). We suggest that RNF212-mediated SUMOylation establishes a precondition for this crossover or noncrossover differentiation process by rendering the turnover of key recombination factors contingent on HEI10-dependent proteolysis. At most recombination sites, HEI10-targeted proteolysis predominates to destabilize nascent intermediates and promote a non-crossover outcome. Designation of a crossover outcome ensues at a minority of sites where RNF212-dependent stabilization predominates, enabling crossover-specific events, including formation of double-Holliday junctions and recruitment of factors such as MutLγ (22). Absent the RNF212-HEI10 pathway, recombination factors that would normally experience transitory stabilization instead turn over more rapidly, crossover designation does not occur, and all DSBs are repaired with a noncrossover outcome.

Our model is consonant with the possibility that HEI10 is a SUMO-targeted ubiquitin ligase (STUbL). Indeed, the RNF212-HEI10 pathway shares general features with STUbL pathways that regulate DSB repair in somatic cells (27). These pathways stall DSB repair at an early step until appropriate features have been installed that minimize aberrant repair (28). We suggest that SUMO conjugation may be a common checkpoint-like mechanism to stall biological processes to enable implementation of important regulatory decisions.

Supplementary Material

Refer to Web version on PubMed Central for supplementary material.

Acknowledgments

We thank A. Gomes, B. de Massy, C. Höög, and V. Dixit for antibodies; M. Paddy for assistance with SIM; and the Hunter Lab for support and discussions. This work was supported in part by National Institute of General Medical Sciences, NIH, grant GM084955. N.H. is an investigator of the Howard Hughes Medical Institute.

REFERENCES AND NOTES

1. Hunter N. Cold Spring Harb Perspect Biol. 2015; 7:a016618. [PubMed: 26511629]
2. Jentsch S, Psakhye I. Annu Rev Genet. 2013; 47:16–86.
3. Eifler K, Vertegaal AC. Trends Biochem Sci. 2015; 40:77–93.
4. Brown PW, Hwang K, Schlegel PN, Morris PL. Hum Reprod. 2008; 23:285–857. [PubMed: 18037605]
5. Watts FZ, Hoffmann E. BioEssays. 2011; 33:52–37. [PubMed: 21110346]
6. Bose R, Manku G, Culty M, Wing SS. Adv Exp Med Biol. 2014; 759:18–13.
7. Jahns MT, et al. PLOS Biol. 2014; 12:e1001930. [PubMed: 25116939]
8. Zhang L, et al. Nature. 2014; 511:55–56.
9. Rodriguez A, Pangas SA. Cell Tissue Res. 2016; 363:4–5.
10. La Salle S, Sun F, Zhang XD, Matunis MJ, Handel MA. Dev Biol. 2008; 321:22–37.
11. Baarends WM, et al. Dev Biol. 1999; 207:32–33.
12. Ahuja JS, et al. Science. 2017; 355:40–11. [PubMed: 28059759]
13. Newton K, et al. Cell. 2008; 134:66–78.
14. La Salle S, Sun F, Handel MA. Methods Mol Biol. 2009; 558:27–97.
15. Kim YS, Nagy K, Keyser S, Schneekloth JS Jr. Chem Biol. 2013; 20:60–13.

16. Yang Y, et al. Cancer Res. 2007; 67:947–481.
17. Syrjänen JL, Pellegrini L, Davies OR. eLife. 2014; 3:e02963.
18. Brockway H, Balukoff N, Dean M, Alleva B, Smolikove S. PLOS Genet. 2014; 10:e1004757. [PubMed: 25375142]
19. Kumar R, Bourbon HM, de Massy B. Genes Dev. 2010; 24:126–280.
20. Brown MS, Bishop DK. Cold Spring Harb Perspect Biol. 2014; 7:a016659. [PubMed: 25475089]
21. Qiao H, et al. Nat Genet. 2014; 46:19–99.
22. Reynolds A, et al. Nat Genet. 2013; 45:26–78.
23. De Muyt A, et al. Genes Dev. 2014; 28:111–123.
24. Cloud V, Chan YL, Grubb J, Budke B, Bishop DK. Science. 2012; 337:122–225.
25. Da Ines O, et al. PLOS Genet. 2013; 9:e1003787. [PubMed: 24086145]
26. Zickler D, Kleckner N. Cold Spring Harb Perspect Biol. 2015; 7:a016626. [PubMed: 25986558]
27. Sriramachandran AM, Dohmen RJ. Biochim Biophys Acta. 2014; 1843:7–5.
28. Freudenreich CH, Su XA. FEMS Yeast Res. 2016; 16:fow095.

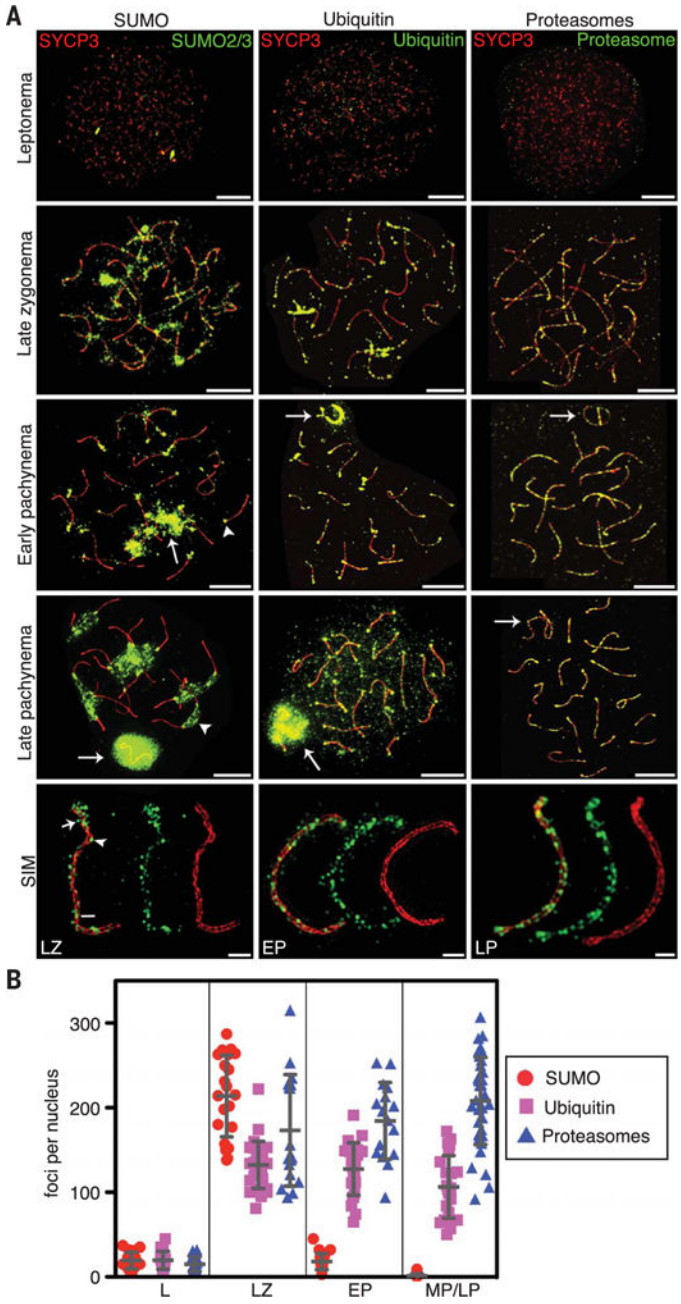

Fig. 1. SUMO, ubiquitin, and proteasomes decorate the axes of meiotic prophase chromosomes

(**A**) Spermatocyte nuclei immunostained for axis marker SYCP3 and SUMO2/3, ubiquitin, or proteasomes. Bottom row shows single chromosomes imaged by SIM. Arrows indicate sex bodies; arrowheads highlight centromeric heterochromatin. In the SUMO2/3 stained SIM image, the arrow, arrowhead, and bar highlight supra-axial, axial, and SC central-region localizations, respectively. Scale bars: 10 μm, wide-field; 1 μm, SIM. (**B**) Quantification of immunostaining foci. L, leptonema; LZ, late zygonema; EP, early pachynema; and MP/LP, mid/late pachynema. Counts from MP and LP nuclei were pooled, as numbers remained stable over these stages. Ubiquitin foci in LP could not be accurately quantified because general chromatin staining obscured axis-specific foci. Error bars show means ± SD.

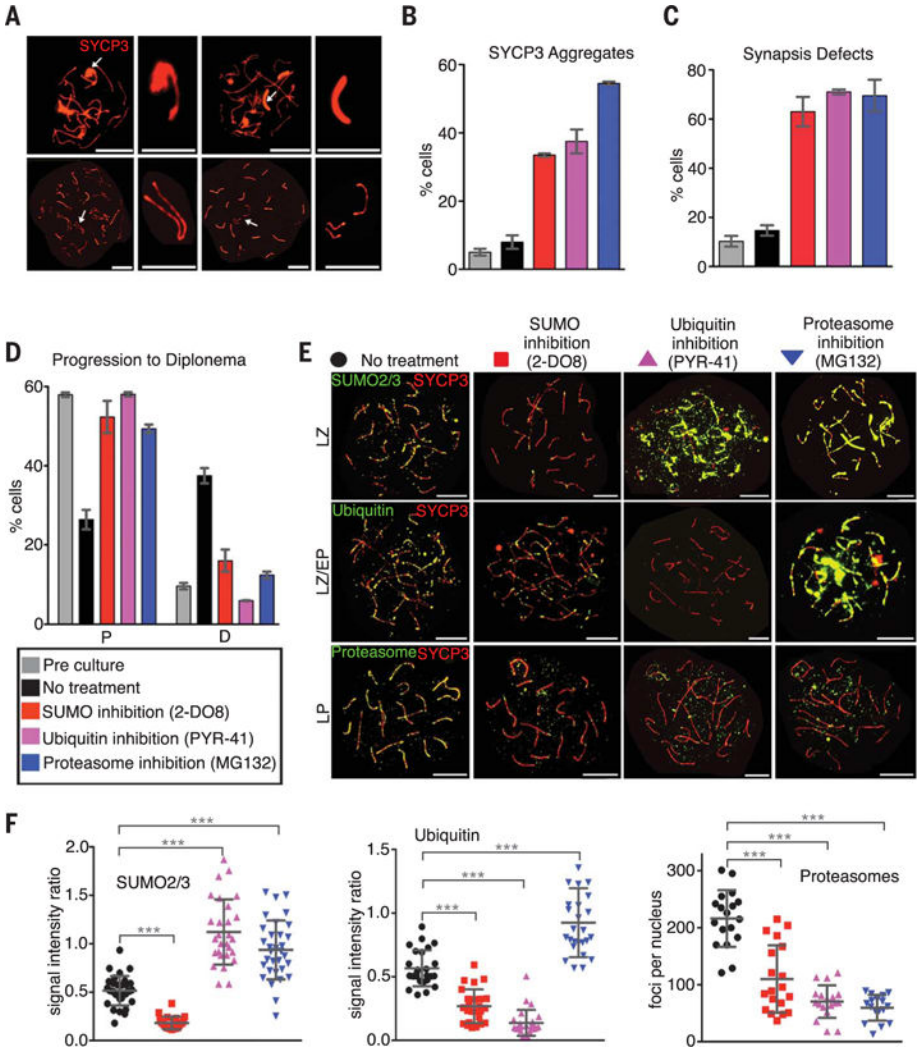

Fig. 2. Interrelated functions of the SMS and UPS in meiotic prophase

(**A**) Pachytene-like spermatocyte nuclei containing SYCP3 aggregates (top) or synapsis defects (bottom). Arrows indicate structures magnified in adjacent panels. (**B** and **C**) Quantification of SYCP3 aggregates (B) and synapsis defects (C). (**D**) Progression of spermatocytes after culture with or without inhibitors. (**E**) Spermatocyte nuclei immunostained for SYCP3 (red) and SUMO2/3, ubiquitin, or proteasomes (green) after chemical inhibition. (**F**) Quantification of experiments shown in (E). Error bars in (B), (C), and (D) show means ± SEM. Error bars in (G) show means ± SD. ***$P \leq 0.001$, two-tailed Mann-Whitney test. Abbreviations as in Fig. 1. Scale bars: 10 μm, full nuclei; 1 μm, magnified structures in (A).

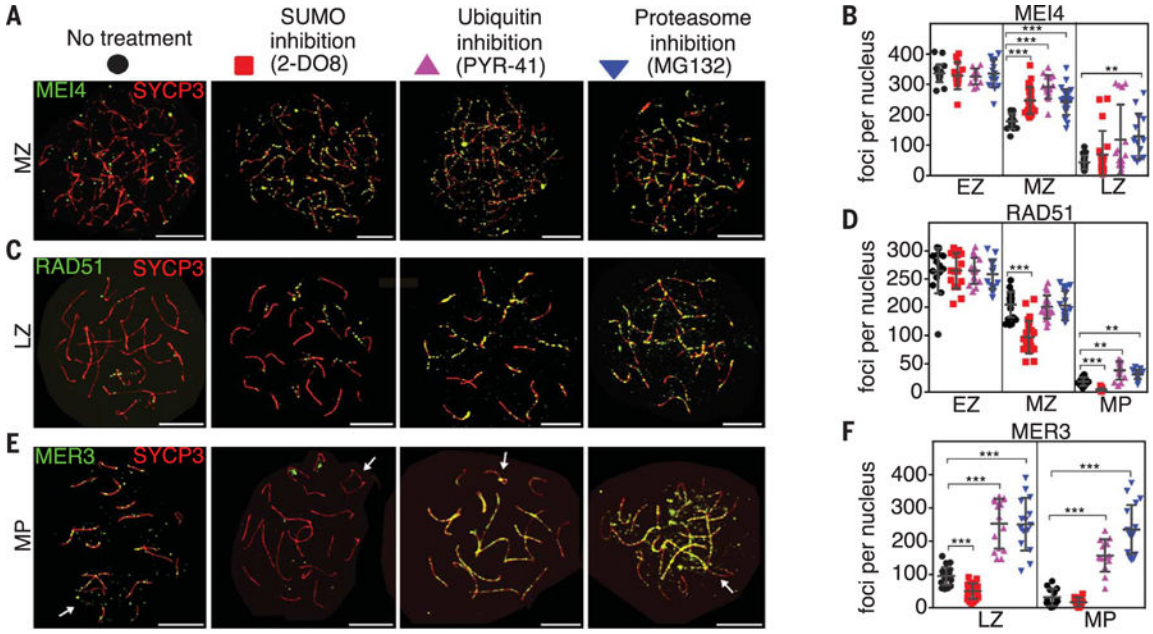

Fig. 3. The SMS and UPS regulate chromosomal dynamics of recombination factors

(**A**, **C**, and **E**) Spermatocyte nuclei immunostained for SYCP3 (red) and MEI4, RAD51, or MER3 (green) following chemical inhibition. (**B**, **D**, and **F**) Quantification of immunostaining foci. Abbreviations as in Fig. 1. Arrows indicate sex chromosomes. Error bars show means ± SD. Scale bars = 10 μm.

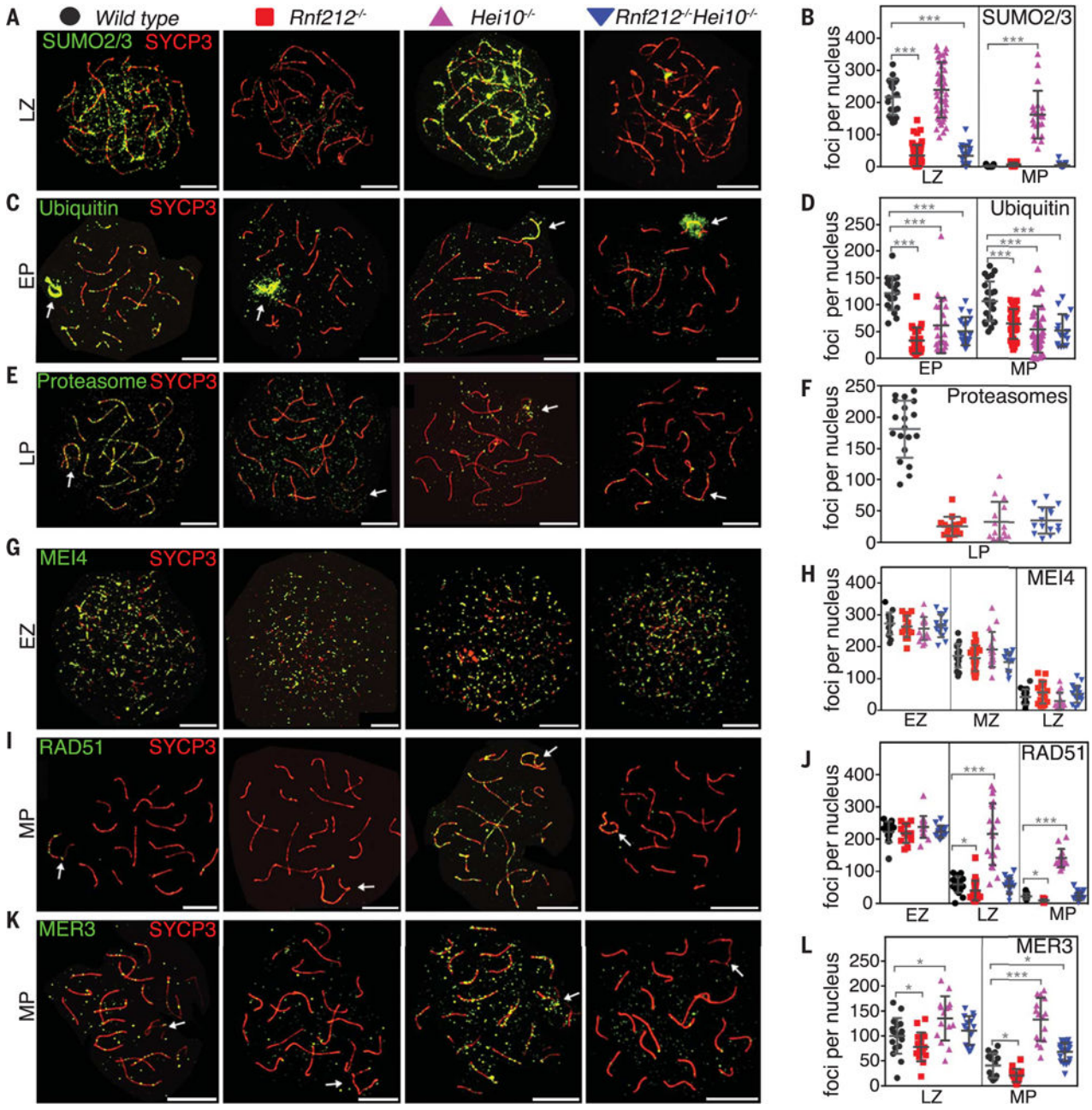

Fig. 4. RNF212 and HEI10 define an axis-associated SUMO-ubiquitin-proteasome relay that regulates turnover of recombination factors

(**A**, **C**, and **E**) Spermatocyte nuclei from indicated strains immunostained for SYCP3 (red) and either SUMO2/3, ubiquitin, or proteasomes (green). See fig. S8 for SUMO1 staining. (**B**, **D**, and **F**) Quantification of immunostaining foci. (**G**, **I**, and **K**) Spermatocyte nuclei immunostained for SYCP3 (red) and MEI4, RAD51, or MER3 (green). (**H**, **J**, and **L**) Quantification of immunostaining foci. EZ, early zygonema; LZ, late zygonema; MP, mid-pachynema. Arrows indicate sex chromosomes. Error bars show means ± SD. *$P \leq 0.05$, ***$P \leq 0.001$, two-tailed Mann-Whitney test. Scale bars, 10 μm.